Journal of Power Sources, *18* (1986) 245 - 258

LIGHTWEIGHT, DIRECT-RADIATING NICKEL–HYDROGEN BATTERIES*

JOHN R METCALFE

Canadian Astronautics Limited, 1050 Morrison Drive, Ottawa, Ont K2H 8K7 (Canada)

Summary

Two battery module configurations have been developed which, in addition to integrating cylindrical nickel–hydrogen ($Ni–H_2$) cells into batteries, provide advances in the means of mounting, monitoring, and thermal control of these cells. The main difference between the two modules is the physical arrangement of the cells· vertical *versus* horizontal. Direct thermal radiation to deep space is accomplished by substituting the battery structure for an exterior spacecraft panel. Unlike most conventional nickel–cadmium (Ni–Cd) and $Ni–H_2$ batteries, the cells are not tightly packed together, therefore ancillary heat conducting media to outside radiating areas, and spacecraft deck reinforcements for high mass concentration, are not necessary.

Testing included electrical characterization and a comprehensive regime of environmental exposures. Despite significant structural differences, the test results were similar for the two modules. High energy density was attained without sacrificing structural rigidity. The results of computer structural analyses were confirmed by a series of vibration tests. Thermal excursions and gradients during geosynchronous orbit (GEO) eclipse day simulations in vacuum were within the nominal range for near optimum $Ni–H_2$ cell performance.

The designs are flexible with respect to quantity and type of cells, orbit altitude and period, power demand profile, and the extent of cell parameter monitoring.

This paper compares the characteristics of the two battery modules and summarizes their performance

Introduction

The Space Systems Group at Canadian Astronautics Limited (CAL) has completed two programs for the design, fabrication, and testing of nickel–hydrogen batteries These were respectively funded under·

*This paper is based on work performed, in part, under the sponsorship and technical direction of the International Telecommunications Satellite Organization (Intelsat) Any views expressed are not necessarily those of Intelsat, or of DOC

0378-7753/86/$3 50

(i) Intelsat Contract-INTEL-151, entitled, "Qualification of an Advanced Nickel Hydrogen Battery", for the R&D Department of the International Telecommunications Satellite Organization.

(ii) Supply and Services Canada contract file no 06ST 36001-3-2410, entitled, "The Enhancement of Advanced Nickel–Hydrogen Battery Technology", for the Communications Research Centre of the Canadian Department of Communications (DOC).

The battery built under the first-mentioned contract is called "IBAT" Figure 1 is a photograph of its spacecraft interior side and Fig. 2 is a photograph of its radiative side This model employs a Crowned Sleeve and Flange cell mounting method whereby the 24 cells pass through the panel with their longitudinal axes normal to the plane of the panel. This was one of the two optimum (energy density *versus* thermal performance and structure strength) concepts of the several candidate layouts analysed during the initial design phase of the Intelsat contract

The alternate concept, named "LYBAT", because the cells "lie down" in the plane of the panel, was not originally chosen for development This was due to the large radiating area needed to handle the peak dissipation of

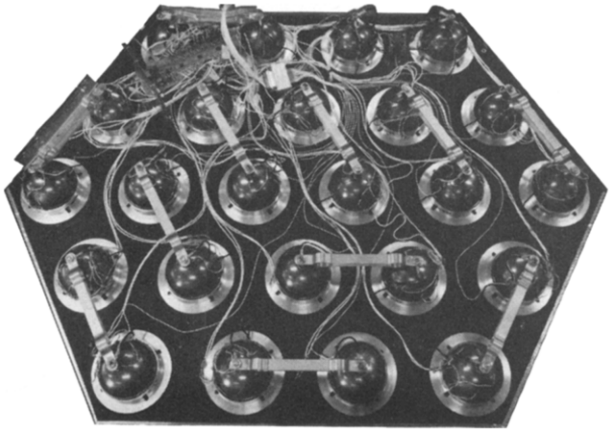

Fig 1 Photograph of underside and monitoring electronics of IBAT

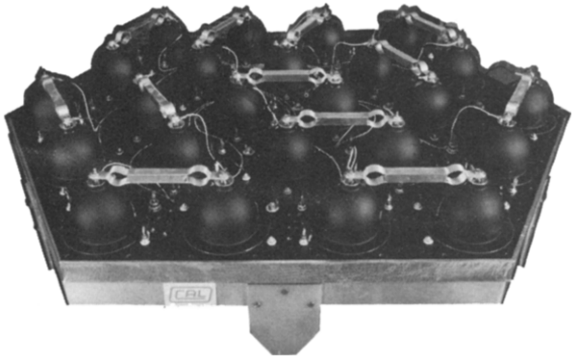

Fig 2 Photograph of radiative side of IBAT

24 cells on a single panel, in view of Intelsat's 80% depth-of-discharge (DOD)/1.2 h eclipse requirement. The LYBAT concept was considered practical, however, for requirements of fewer cells per "pack" or for lower DODs The major requirement of the second contract was the accommodation of 9 cells lying in the plane of the radiating support plate. Figure 3 is a photograph of the LYBAT prototype interior side and Fig 4 is a photograph of its radiative side.

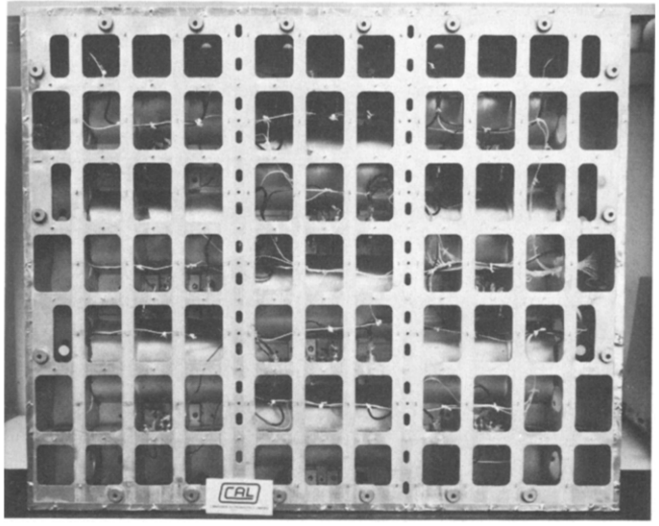

Fig 3 Photograph of the LYBAT prototype interior side

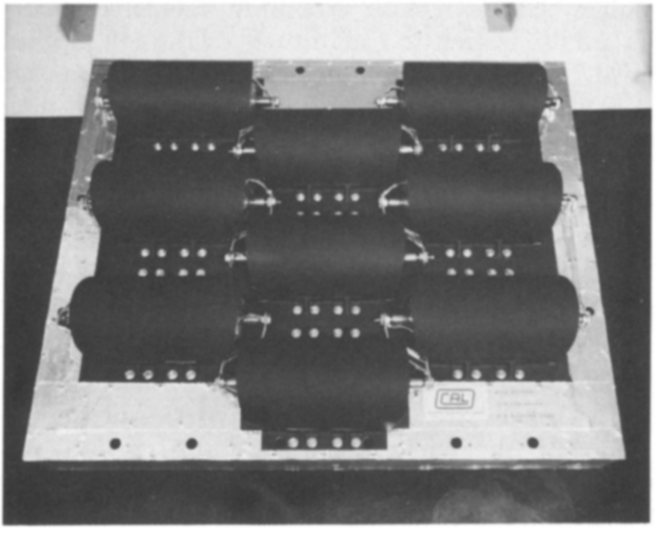

Fig 4 Photograph of the LYBAT prototype radiative side

Cells

Both battery modules employ 3 5 in dia. "Intelsat design" cells of 50 A h nameplate capacity (Yardney model YNH50-5). However, both designs can accommodate larger, longer and/or heavier, individual pressure vessel (IPV) cells, including the new generations of very high energy 3 5 in and 4 5 in cells Both designs can be used in GEO and low earth orbit (LEO) applications. In addition, the LYBAT mounting system lends itself particularly well to common pressure vessel (CPV) cells of considerably greater length

Battery characteristics

Table 1 compares the characteristics of the two units in summary form.

Mechanical and thermal design

Both projects involved extensive use of stress analysis and thermal modelling to determine the optimum structure configurations and dimensions Experiments were also carried out to evaluate materials and fastening/mounting techniques.

Panel structures

IBAT The IBAT was built employing a single, hexagonal-shaped sheet of 1 5 in. thick standard aerospace honeycomb panel to support the 24 cells and all of the associated hardware Panel holes for components and fasteners were cut and later edge strengthened

LYBAT. LYBAT employs a structure believed to be unique in the battery field It is an "egg-crate" lattice of sheet aluminum web pieces, many as thin as 0 016 in , which are dip-brazed to each other, to the cell support saddles, and to the radiative face skin. Various forms of support brackets and strengthening techniques were utilized.

Cell mounting

IBAT The 24 IBAT cells are retained by through-plate mounts incorporating precision machined sleeves, flanges, and crowns (Fig 5(a)) Each cell is bonded to the sleeve with a flexible, thermally-conductive adhesive using special techniques to align the cell in its sleeve. A locking mechanism then assures a strong bond to the panel itself Each cell assembly radiates directly to the external environment.

LYBAT The nine LYBAT cells are seated in formed saddle sections which are recessed part way into the 2.5 in. deep support structure (Fig 5(b)). The cell covers are bolted to the panel via braces above and below the face skin, the cell having been bonded to the assembly in a manner similar to that of IBAT

TABLE 1

Comparison of the characteristics of direct-radiating $Ni-H_2$ batteries

Model	"LYBAT"	"IBAT"
Structure	Dip-brazed lattice	Al honeycomb
Cell mounting	Saddles in plane of panel	Crowned sleeve and flange, through panel
Cell type	50 A h nameplate "Intelsat design"	50 A h nameplate "Intelsat design"
Cell quantity	9	24
Panel shape	Rectangular	Hexagonal
Footprint area	2 635 ft^2/0 245 m^2 42 2 in^2 per cell	7 079 ft^2/0 658 m^2 42 5 in^2 per cell
Mass	13 3 kg net	37 3 kg net
Capacity	51 6 A h (10 °C)	51 5 A h (10 °C)
Energy	560 W h (10 85 V)	1483 W h (28 8 V)
Energy density	42 1 W h kg^{-1} net	39 8 W h kg^{-1} net
Projected E D 75 A h cells	46 5 W h kg^{-1} (see Fig 6)	46 0 W h kg^{-1} (see Fig 6)
Vibration test	Survived sine and random tests (3 axes)	Survived sine and random tests (3 axes)
Structure resonances	>150 Hz	>85 Hz
Discharge current ratings	25 A nom 36 A max 150 A surge	33 3 A nom 36 A max 150 A surge
Built-in monitoring	Temperatures, cell voltages	Cell pressures, cell voltages
Protection	Redundant connections diode bypasses	Redundant connections diode bypasses
Heat output	Radiation to space	Radiation to space
Heat input	Electric heaters during insolation	Electric heaters during insolation
Equilibrium temperature	7 ± 3 °C	13 ± 3 °C
Thermal gradients	<6 5 °C intercell (<5 °C capability) < 10 °C cell int	<10 °C intercell (<4 °C capability) <10 °C cell int

End-domes Cell vessel end-domes for both batteries were fitted with thermal insulation prior to installation. This was to prevent excessive cooling of end-domes located on the "space" side of the panels.

Safety For safety reasons, the cells for both batteries were conformally coated prior to installation. The thin layer of urethane has negligible effect on heat transfer, but prevents accidental electrical contact from the cell vessel with other metal parts. Despite the relatively high impedance between a cell's case and its power path, it is known that a small intermittent contact point from a vessel with its mounting hardware (near negative battery terminal potential) can, with the battery fully charged, spark-erode an orifice through the Inconel wall of the pressure vessel, releasing hydrogen.

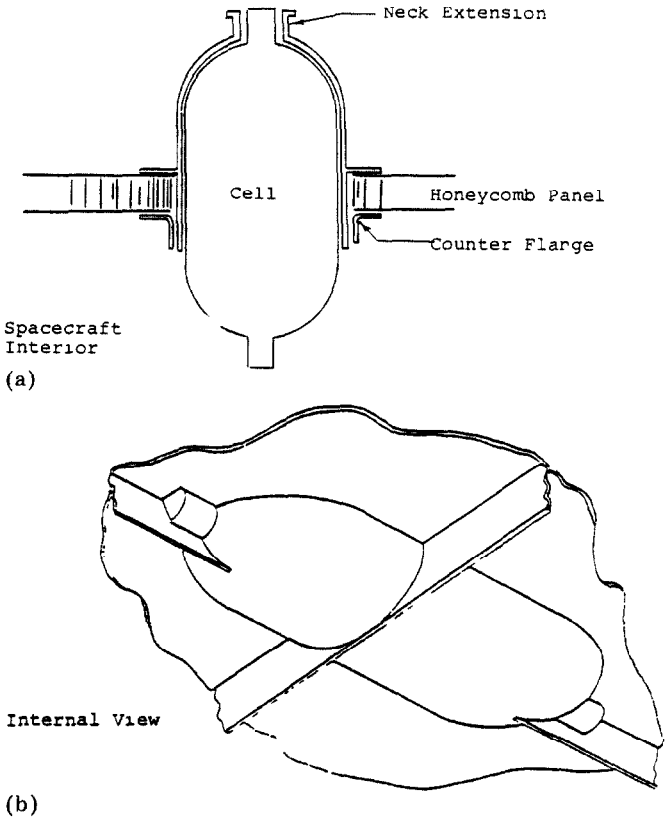

Fig 5 (a) Cell mounting of IBAT Cells are retained by through-plate mounts incorporating precision machined sleeves, flanges and crowns (b) Cell mounting of LYBAT Cells are seated in formed saddle sections which are recessed part way into the support structure

Temperature gradients

A basic design goal was the minimization of intercell and internal cell temperature gradients, the former to within 5 °C for prevention of temperature driven imbalances in cell capacities, and the latter to within 10 °C (core to vessel) to prevent vapour transfer from the electrolyte to the inner wall of the cell vessel. Attention was paid to balancing the thermal conductivities of the cell mounting hardware Transient thermal analyses were carried out to predict gradients from the effects of cell dissipations during an eclipse.

Cell spacing/Surface area The distance between cell locations, which reflects directly upon volumetric energy density and occupied footprint area, was determined mainly by the panel area per cell required to augment the cell covers' ability to dissipate peak cell dissipation with acceptable temperature gradients This was established by iterative analyses of the computer models. The practical constraints of structure/fastener interfacing also played a role

If designed for the same dissipation levels, the IBAT technique is inherently smaller than the LYBAT in footprint area per cell However, the IBAT was built for an approximately 60% higher peak cell dissipation. This resulted in the per cell footprint areas being nearly identical for the as-built models

Thermal aspects — LEO

The present limits of continuous discharge current, with respect to dissipation handling, are. LYBAT — 33.3 A for 36 min or 25 A for 72 min; IBAT — 36 A for 72 min.

The LYBAT thermal analysis was extrapolated for the higher current, shorter duration charge/discharge regime of a typical 110 min orbit, LEO application The main problem area is the high cell dissipation encountered at end of charge, just prior to eclipse commencement If charge return ratios were balanced accordingly, and if cells with higher stack-to-shell thermal conductivity were employed, discharge rates of 50 - 60 A could be safely maintained during a 36 min eclipse period with few design alterations. A similar prospect is foreseen for the IBAT design.

Electrical design

Electrical design made use of tolerance, stress and failure mode analyses, along with mass *versus* power loss tradeoff studies, to choose the methods and piece parts for the power paths, the main power connector interfaces, the cell bypass circuits, and the sensor circuits for monitoring of temperatures, cell pressure, and cell voltages.

Power path Both models employed special lightweight, low-loss cell interconnects, which proved to be superior to copper wire. Wiring was used to connect the ends of the series cell strings to the main power connectors and to connect the cell bypass circuits The IBAT has a single main power connector The LYBAT has two separate power connectors to facilitate series interconnection, with identical modules on adjacent panels, to attain a battery with any multiple of nine cells

Cell bypass circuits The familiar method of open-circuit protection; three series diodes per cell for charge and one, larger power diode per cell for discharge, was employed. These diodes were located to minimize thermal imbalance effects, should they become activated

Because of the higher currents involved in a typical LEO application, the mass of the larger power rectifiers required, and their potentially high dissipations, would be prohibitive. High current aerospace relays are also relatively heavy. To increase battery energy density, special development of a low mass sense switch, designed for one closure operation across a failed cell, may be the solution for both GEO and LEO batteries

Monitoring circuits Both batteries have isolated voltage sense lines from cell terminals to a monitoring harness connector In addition, the LYBAT has four permanent temperature transducers (two on cells, two on panel structure) which are monitored via the same connector.

Pressure monitoring The IBAT has a specially developed, on-board strain gauge processor (SGP), which selects the strain gauge bridge reading for the desired cell, amplifies it and transmits it to the ground station via spacecraft telemetry The SGP entails a low-power module, containing two small circuit cards, on the spacecraft interior side of the battery panel (Fig 1) Integrated circuits were chosen on the basis of their availability in radiation hardened versions

The SGP and strain gauge bridge wiring are relatively low in mass, as depicted by the proportion of monitoring circuits' mass in Fig 6, and they provide an indication of state of charge

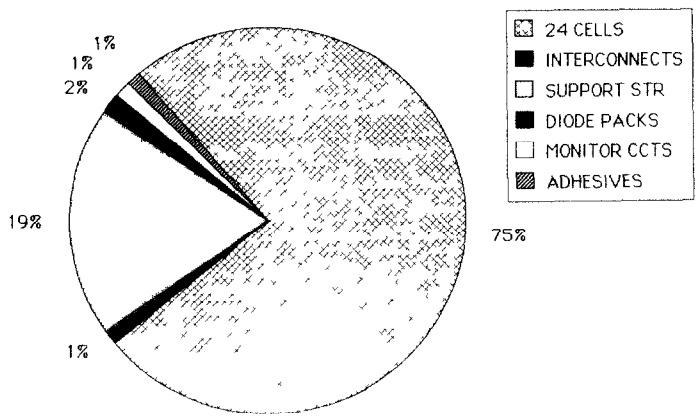

Fig 6 Breakdown, in percent , of the mass of the components of IBAT

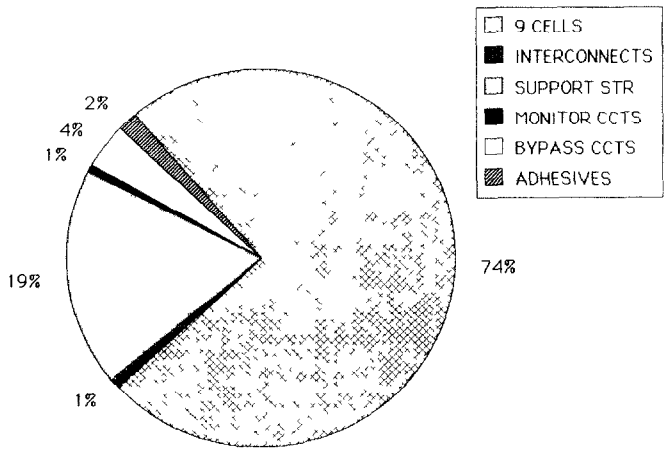

Fig 7 Breakdown, in percent , of the mass of the components of LYBAT

Figure 7 illustrates the percentages of LYBAT's mass components Figures 8 and 9 depict actual SGP cell pressure data and voltage of the same IBAT cell for a charge/discharge cycle at 10 °C.

Testing

The test results and other performance data, including projections for an advanced cell type, are summarized in Table 1. The test equipment used at

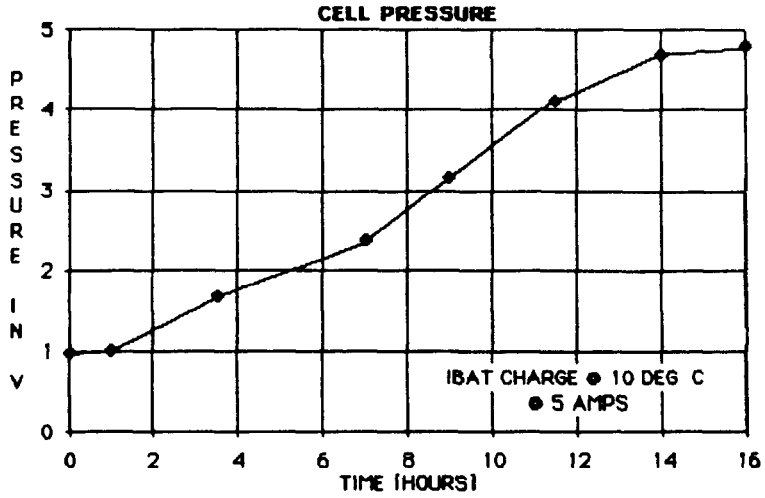

(a)

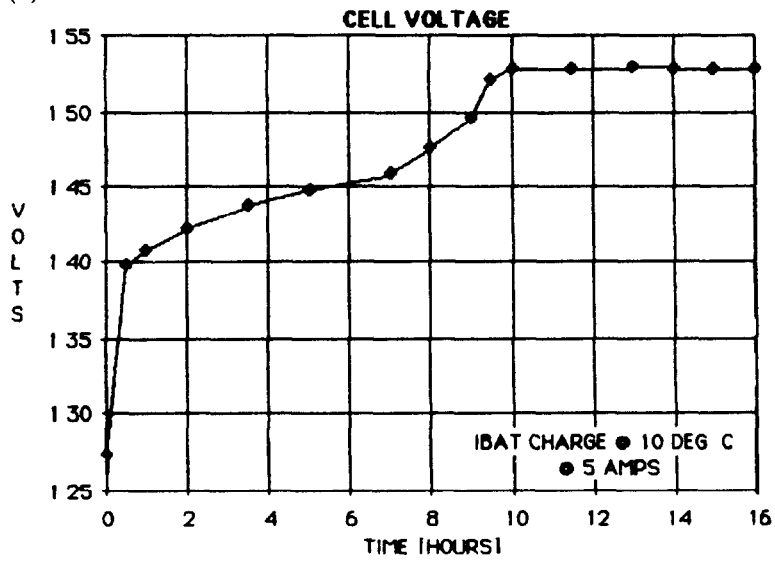

(b)

Fig. 8 IBAT strain gauge processor (SGP) data for (a) cell pressure, (b) cell voltage. Temperature 10 °C, charge 5 A

CAL for electrical and thermal control (in air) of the batteries is shown in Fig 10

Capacity

Battery capacities were determined from the time taken to reach an end of discharge voltage (EODV) equal to the number of cells times 1.00 V, at a constant current of 25.0 A Reference capacities were recorded during the last cycle of several overcharge/one hour stand/discharge sequences, at the

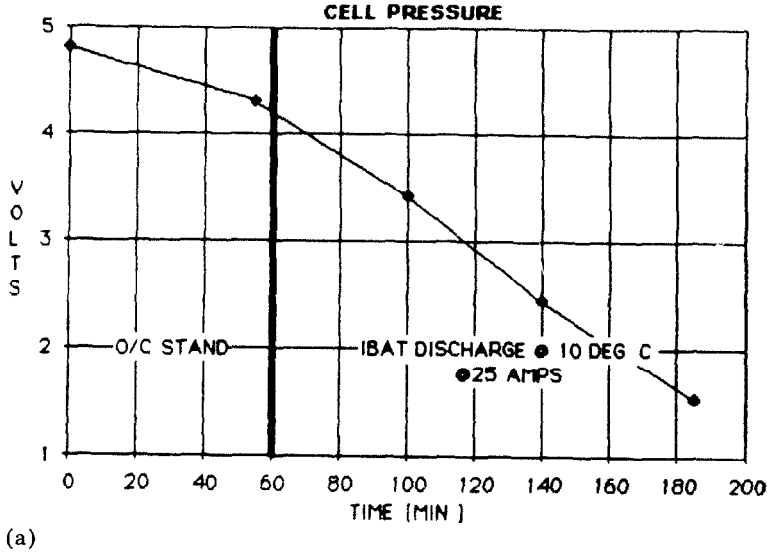

(a)

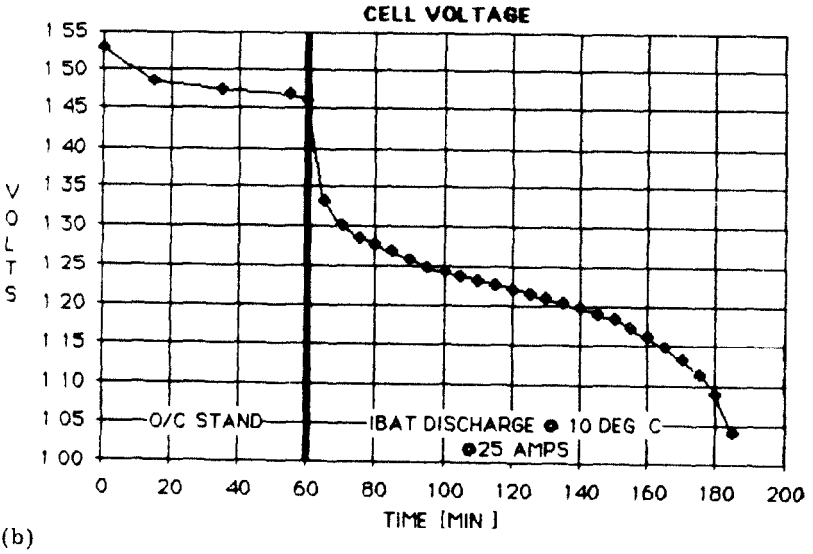

(b)

Fig 9 IBAT strain gauge processor (SGP) data for same cell as Fig 8, showing (a) cell pressure, (b) cell voltage during open circuit stand and 25 A discharge at 10 °C

Fig 10 Test equipment used at CAL for electrical and thermal control, in air, of batteries

reference temperature of 10 ± 3 °C Both batteries had typical capacities of 52 ± 1 A h.

Energy density

IBAT

The mass of the IBAT module is 40.0 kg After deducting the predetermined replaced structure allowance, the net mass is 37.3 kg, for an energy density of 39 8 W h kg^{-1}, based on 51.5 A h capacity with a mid-discharge voltage of 28.8 V

LYBAT

The mass of the LYBAT module, not including 0.4 kg of extra adhesives and brackets added to correct two minor problems (easily resolvable in a future model), is 14.8 kg. After deducting the predetermined replaced structure allowance, the net mass is 13.3 kg, for an energy density of 42.1 W h kg^{-1}, based on 51.6 A h capacity with a mid-discharge voltage of 10.85 V.

Comparisons

Figure 11 compares the energy densities of conventional "close-packed" 35 A h and 40 A h Ni–H_2 batteries with those of the IBAT and LYBAT, and with the projected energy densities for the as-built IBAT minus the mass of pressure monitoring apparatus, and for the IBAT and LYBAT concepts using 75 A h cells typical of those now nearing fully developed status

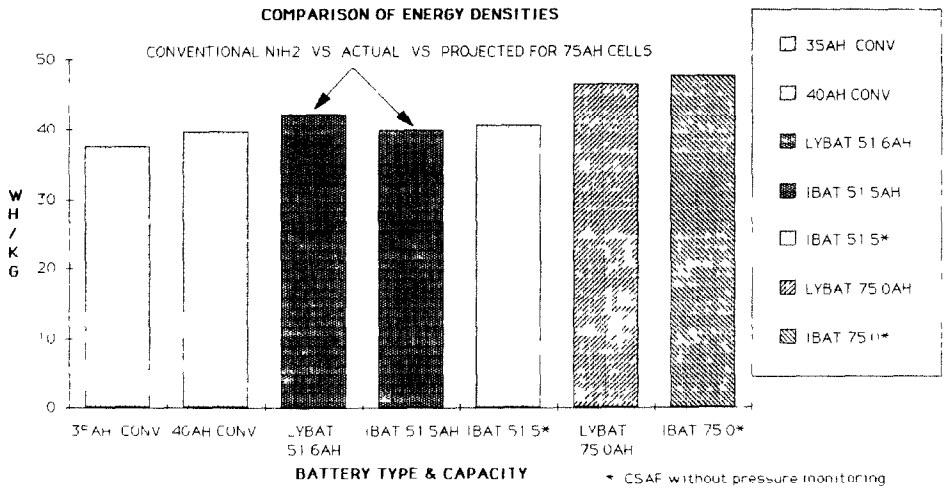

Fig 11 Comparison of the energy densities of conventional "close-packed" 35 and 40 A h batteries with those of IBAT and LYBAT, with the projected energy densities for the as-built IBAT minus the mass of pressure monitoring apparatus, and for the IBAT and LYBAT concepts using 75 A h cells
*CSAF without pressure monitoring

Although the energy density of the LYBAT appears to be significantly greater than that of IBAT, the total weight per cell of the former is only 22 g less Additional mass saving measures are already assured for future models

Electrical and thermal cycling

IBAT The IBAT successfully underwent a regime of extreme temperature excursions (in air) while electrically active at test temperatures ranging from −15 to +40 °C In addition, reference cycling was done for capacity determination at 0, 10, 20, and 30 °C, and test stages were interspersed with capacity retention tests at 10 °C to check for degradation

LYBAT LYBAT's testing in air was limited to characterization cycling at 10 °C and a capacity determination at 25 °C (46.6 A h). Power losses in the cell interconnects (bus bars) were measured to be only 3.3 W at 25 A.

Vibration testing

One-piece machined mounting fixtures were used to mount the batteries for vibration testing The facilities of the David Florida laboratory, located at the Communications Research Centre near Ottawa, were employed An input spectrum, derived from a combination of available launch vehicle data (Delta/Shuttle/Ariane), was applied in the three orthogonal axes, in both random and swept sinusoidal modes

The structures of both modules were successfully vibration tested to the limits specified for the cells. Force levels experienced by the cells were up to 13 *g*-rms in random mode, and 20 *g*-peak in sinusoidal mode Panel

resonances were slightly above the predicted frequencies, indicating that the intended stiffness had been achieved. The results supported the findings of the structural analyses, which predicted high stress capabilities at high confidence levels.

Thermal vacuum testing

Again at the David Florida Laboratory Space Simulation Facility, the batteries were tested in thermal vacuum at pressures less than 1×10^{-6} Torr The set-ups involved enclosing the battery undersides and resistive heaters with insulating material to simulate the interior of the spacecraft Thermocouples were placed at strategic locations. The chamber walls were cooled with liquid nitrogen to approximate deep space temperatures

A GEO full-eclipse day simulation was run for each battery Figure 12 illustrates the actual average cell temperature profiles through eclipse (discharging at 25 A) Intercell temperature gradients were within the design maximum range, and internal cell gradients (stack to vessel differential) were determined, by analysis of measured *versus* predicted node temperatures, to be within the safe operational range

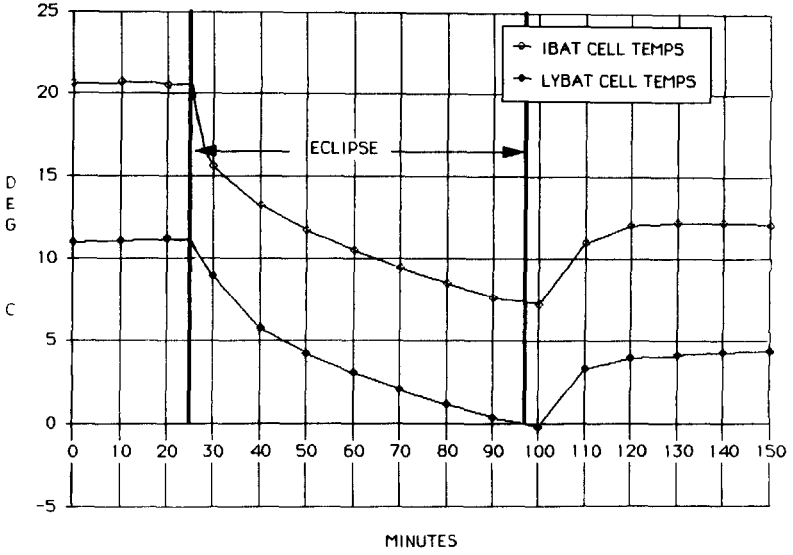

Fig 12 GEO full eclipse day simulation for IBAT and LYBAT Actual average cell temperature profiles through eclipse, discharging at 25 A

Conclusion

Two lightweight support structures and cell mounting systems have been shown to be feasible for serious consideration in future spacecraft energy storage systems. Substitution of exterior, or space-viewing, panel

sections not only saves the mass of the obviated panel, but liberates internal space for payload use The layouts are adaptable to a variety of panel sizes and shapes, and to the voltage and power profile requirements of many communications, remote sensing and scientific satellites

Acknowledgements

The author expresses his appreciation of the front-end design and organizational work by Mr Malcom H Moody, of CAL.

These two projects have enabled CAL to establish a firm base in Ni–H_2 technology We gratefully acknowledge the support and responsiveness of our customers' scientific authorities Dr John Stevenson of Intelsat and Mr George Mackie and Dr Don Edwards of Communications Canada